Line strengths, N_2-, and O_2-broadened half-widths in the $\nu_1+\nu_3$ band of $^{14}N_2{}^{16}O$ at room temperature

M. Fukabori,[1] T. Aoki,[1] and T. Watanabe[2]

[1] *Meteorological Research Institute, 1-1 Nagamine, Tsukuba, Ibaraki 305-0052, Japan*
[2] *Toray Research Center Inc., 3-3-7 Sonoyama, Otsu, Shiga, 520-8567, Japan*

Received December 27, 2002

Line strengths, N_2-, and O_2-broadened half-widths in the $\nu_1 + \nu_3$ band of $^{14}N_2{}^{16}O$ were determined from spectra obtained by a high-resolution Fourier transform spectrometer at room temperature. The square of the transition dipole moment matrix element and the coefficients of the Herman–Wallis factor were also determined for this band. The values of measured line strengths are close to those of HITRAN92 rather than those of HITRAN96 and HITRAN2K. The N_2- and O_2-broadened half-widths measured in this study were in good agreement with the results of the recent high-resolution experiments by other researchers. Air-broadened half-widths were derived from N_2- and O_2-broadened half-widths smoothed by a polynomial fit.

Introduction

Nitrous oxide (N_2O) is an important greenhouse gas in the Earth's atmosphere. The very strong infrared absorption bands of the ν_3 and ν_1 fundamental bands at 4.5 and 7.78 μm, respectively, are important for the study of the thermal balance in the terrestrial atmosphere. Remote sensing measurements of N_2O in the stratosphere have been used for the research of the stratospheric chemistry related to ozone depletion. Accurate knowledge of the absorption line parameters such as the line strengths and half-widths of the absorption bands of N_2O is required for the calculation of the atmospheric transmittance. Several spectroscopic databases are available for this purpose. The HITRAN databases[1–4] are widely used to calculate the spectra, but the accuracies of the compiled values in HITRAN could still be insufficient for the purposes of accurate remote sensing.

There exist several absorption bands of N_2O in the 2.9 μm region; the $\nu_1 + \nu_3$ band centered at 3480.821 cm^{-1} is the strongest band in the 2.9 μm region. The $\nu_1 + \nu_3$ band of $^{14}N_2{}^{16}O$ is important because it is used for temperature remote sensing. It also contributes to the thermal balance of the Earth's atmosphere. Extensive experimental studies[5–14] for the infrared absorption bands of N_2O have been carried out to determine the line parameters. The line and band strengths of the $\nu_1 + \nu_3$ band of $^{14}N_2{}^{16}O$ were reported in Refs. 5–8, and the N_2- and O_2-broadened half-widths of the infrared absorption bands of $^{14}N_2{}^{16}O$ were reported in Refs. 9–14. On the basis of these experimental studies, the spectroscopic databases were revised several times. However, the line strengths of this band were not revised from the initial version of the AFCRL line compilation[1] until the HITRAN96[3] database. At the HITRAN96[3] database, the line strengths of this band were updated and the same values were compiled in HITRAN2K.[4] For the $\nu_1 + \nu_3$ band of $^{14}N_2{}^{16}O$, the line strengths of HITRAN96,[3] 2K,[4] which are based on the high-resolution experiments by Toth,[7] are about 4% larger than those of HITRAN92.[2] In order to validate the compiled values in the HITRAN databases, we determined the line strengths, N_2-, and O_2-broadened half-widths in the $\nu_1 + \nu_3$ band of $^{14}N_2{}^{16}O$ at room temperature. The results obtained in this study were compared with the HITRAN databases and others previously reported in the literature.

Experimental details and data analysis

All the spectra were measured using a high-resolution Fourier transform spectrometer (Bruker IFS 120HR) with a resolution of 0.01 cm^{-1}. One spectrum was obtained with a pure N_2O sample and four spectra were obtained with mixtures of N_2O in N_2 and O_2. Experimental conditions are listed in Table 1. All the measurements were performed using an 8.75-cm-length cell with ZnSe windows at 297.5 K. The sample temperature was measured with the thermocouples and the variation of the temperature was kept within 1 K during the measurements. Sample pressures were measured with an MKS Baratron pressure gauge of the 1000-Torr head. The signal to noise ratios of the spectra were better than 500.

Table 1. Experimental conditions

$P(N_2O)$, Torr	$P(N_2)$, Torr	$P(O_2)$, Torr	Temperature, K
15.2	0.0	0.0	297.5 ± 1
15.2	136.8	0.0	297.5 ± 1
15.2	364.8	0.0	297.5 ± 1
15.2	0.0	136.8	297.5 ± 1
15.2	0.0	364.8	297.5 ± 1

A nonlinear least-squares fitting technique was adopted to determine the line strengths as well as the N_2- and O_2-broadened half-widths. The Voigt profile was assumed as a line shape. The square of the transition dipole moment matrix element and the

coefficients of the Herman–Wallis factor were also determined using the least-squares method. The analysis of the pressure-induced line shifts is in progress.

The individual line strengths S_i are expressed by the following formula:

$$S_i = \{8\pi^3 \cdot 10^{-36} / [3hcg_V Q_V Q_R]\} \times$$
$$\times \{\nu_i f \exp[-(E_V + E_R)hc/kT]\} L_i |R_V|^2 F \times$$
$$\times [1 - \exp(-hc\nu_i/kT)], \quad (1)$$

where $|R_V|^2$ is the square of the transition dipole moment matrix element, L_i is the Hönl–London factor, ν_i is the line position, $f = 0.9903$ is the isotopic abundance for $^{14}N_2{}^{16}O$, g_V is the degeneracy factor, Q_V and Q_R are, respectively, the vibrational and rotational partition functions, E_V and E_R are, respectively, the lower state vibrational and rotational energy levels, F is the Herman–Wallis factor (F-factor), T is the temperature, h is the Planck constant, k is the Boltzmann constant, and c is the speed of light in vacuum. The line strength is given in units of $cm^{-1}/(molecule/cm^2)$ and the square of the transition dipole moment matrix element is in Debye.[2]

The expression of the Herman–Wallis factor, which allows for vibration-rotation interaction on the line strengths, is given for the R and P branches

$$F(m) = (1 + A_1 m + A_2 m^2)^2, \quad (2)$$

where the running index $m = J'' + 1$ for the R-branch and $m = -J''$ for the P-branch, and J'' is the lower-state rotational quantum number.

The measured line strength and half-width γ^0 were, respectively, converted to the reference temperature of $T = 296$ K by using the following relations

$$S(T_s) = S(T)\,[T\,Q_V(T) \times$$
$$\times \exp(-E_R hc/kT)]/[T_s Q_V(T_s) \exp(-E_R hc/kT_s)] \quad (3)$$

and

$$\gamma^0(T_s) = \gamma^0(T)\,(T/T_s)^n. \quad (4)$$

In Eq. (3), $S(T)$ is the measured line strength at T and $S(T_s)$ is the line strength at the reference temperature T_s. The values of Q_V (296 K) = 1.127 and Q_V (297.5 K) = 1.129 were used from Ref. 15. In Eq. (4), $\gamma^0(T)$ is the measured half-width at T and $\gamma^0(T_s)$ is the half-width at the reference temperature T_s. The temperature dependence exponent n of the half-width was assumed to be 0.75.

Results and discussion

1. Line strengths

No systematic discrepancy has been found between the sets of line strengths deduced from the self-, N_2-, and O_2-broadening experiments. Figure 1 shows the comparison of the measured line strengths with the values of the HITRAN databases. The line strengths at 296 K are listed at the third column in Table 2. The uncertainties of measured quantities given in parentheses in Table 2 correspond to one standard deviation in units of the last quoted digit. For the $\nu_1 + \nu_3$ band of $^{14}N_2{}^{16}O$, the line strengths obtained in this study agreed well with the values of HITRAN92,[2] which were the same as the values of AFCRL line compilation,[1] rather than those of HITRAN96[3] and HITRAN2K.[4] The line strengths compiled in the HITRAN96,2K databases are based on the results of recent high-resolution experiments by Toth.[7]

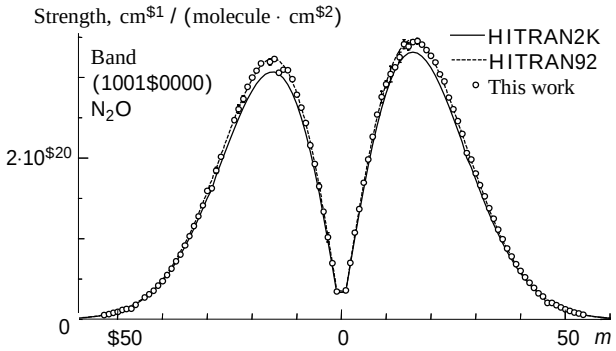

Fig. 1. Comparison of the line strengths measured in this study with those of the HITRAN databases.

Table 2. The line strengths, N_2-, and O_2-broadened half-widths for the $\nu_1 + \nu_3$ band of $^{14}N_2{}^{16}O$

m	ν, cm^{-1}	S, $cm^{-1}/(molecules \cdot cm^{-2})$	$\gamma^0(N_2)$, cm^{-1}/atm	$\gamma^0(O_2)$, cm^{-1}/atm
−53	3422.140978	5.497(810)E−22*	0.0804(52)	0.0863(81)
−52	3423.513752	6.473(678)E−22	0.0629(37)	0.0709(175)
−51	3424.876347	8.055(763)E−22	0.0697(30)	0.0691(52)
−50	3426.228598	9.312(998)E−22	0.0724(93)	0.0640(128)
−49	3427.570554	1.161(83)E−21	0.0688(88)	0.0531(63)
−48	3428.900753	1.297(39)E−21	0.0700(21)	0.0601(37)
−47	3430.202512	1.324(51)E−21	0.0740(41)	0.0647(37)
−46	3431.548011	1.796(112)E−21	0.0716(42)	0.0624(45)
−45	3432.846259		0.0682(15)	0.0581(18)
−44	3434.137244	2.711(80)E−21	0.0705(32)	0.0616(44)
−43	3435.418635	3.109(64)E−21	0.0664(26)	0.0653(85)
−42	3436.690154	3.573(14)E−21	0.0705(91)	0.0729(0)
−41	3437.951438	4.189(97)E−21	0.0697(24)	0.0711(166)
−40	3439.202739	4.736(65)E−21	0.0714(13)	0.0606(20)

Table 2 (continued)

m	ν, cm^{-1}	S, $cm^{-1}/(molecules \cdot cm^{-2})$	$\gamma^0(N_2)$, cm^{-1}/atm	$\gamma^0(O_2)$, cm^{-1}/atm
−39	3440.443867	5.516(56)E−21	0.0716(7)	0.0609(12)
−38	3441.674832	6.283(61)E−21	0.0727(11)	0.0620(17)
−37	3442.895575	7.230(97)E−21	0.0733(12)	0.0627(22)
−36	3444.106147	8.060(95)E−21	0.0730(20)	0.0619(25)
−35	3445.306330	9.172(100)E−21	0.0728(15)	0.0619(22)
−34	3446.496494	1.033(67)E−20	0.0733(11)	0.0622(13)
−33	3447.676411	1.158(83)E−20	0.0733(13)	0.0622(15)
−32	3448.846073	1.280(86)E−20	0.0730(9)	0.0616(13)
−31	3450.005372	1.413(75)E−20	0.0742(11)	0.0627(13)
−30	3451.154300	1.596(12)E−20	0.0740(2)	0.0627(17)
−29	3452.295089	1.628(18)E−20	0.0747(0)	0.0628(0)
−28	3453.422192	1.845(37)E−20	–	–
−27	3454.540282	2.018(20)E−20	–	–
−26	3455.648250	–	–	–
−25	3456.745910	–	–	–
−24	3457.833255	2.474(18)E−20	0.0766(24)	0.0649(27)
−23	3458.910279	2.607(50)E−20	0.0748(2)	0.0649(19)
−22	3459.976974	2.733(40)E−20	0.0759(17)	0.0637(11)
−21	3461.033334	2.885(10)E−20	0.0776(10)	0.0664(15)
−20	3462.079353	3.000(18)E−20	0.0780(11)	0.0672(13)
−19	3463.115024	3.087(16)E−20	0.0778(20)	0.0669(22)
−18	3464.140341	3.175(33)E−20	0.0798(22)	0.0677(33)
−17	3465.155298	–	–	–
−16	3466.159890	3.193(39)E−20	–	–
−15	3467.154110	3.230(27)E−20	–	–
−14	3468.137952	3.058(14)E−20		0.0732(38)
−13	3469.111412	3.096(18)E−20	0.0836(25)	0.0726(27)
−12	3470.074484	3.090(19)E−20	0.0839(23)	0.0730(26)
−11	3471.027162	2.979(19)E−20	0.0846(18)	0.0739(22)
−10	3471.969441	2.786(15)E−20	0.0856(17)	0.0748(21)
−9	3472.901316	2.626(26)E−20	0.0887(24)	0.0777(25)
−8	3473.822781	2.434(19)E−20	0.0875(17)	0.0772(20)
−7	3474.733833	2.159(18)E−20	0.0897(18)	0.0789(23)
−6	3475.634465	1.926(17)E−20	–	–
−5	3476.524674	1.649(42)E−20	–	–
−4	3477.404454	1.336(12)E−20	0.0914(0)	–
−3	3478.273802	1.018(57)E−20	0.0917(4)	–
−2	3479.132711	6.943(112)E−21	0.0961(9)	–
−1	3479.981179	3.453(45)E−21	0.0105(0)	–
1	3481.646771	3.576(40)E−21	0.0997(17)	–
2	3482.463887	6.978(16)E−21	0.0100(41)	–
3	3483.270544	1.075(16)E−20	–	–
4	3484.066739	1.367(15)E−20	0.0936(21)	0.0830(23)
5	3484.852467	1.695(14)E−20	0.0904(13)	0.0803(18)
6	3485.627725	1.982(15)E−20	0.0885(10)	0.0779(15)
7	3486.392509	2.264(22)E−20	0.0883(15)	0.0775(19)
8	3487.146815	2.540(12)E−20	0.0839(9)	0.0734(1)
9	3487.890641	2.759(72)E−20	–	–
10	3488.623982	2.916(43)E−20	0.0812(11)	–
11	3489.346835	3.041(97)E−20	0.0813(8)	0.0713(2)
12	3490.059198	3.126(17)E−20	0.0805(26)	0.0703(19)
13	3490.761066	3.251(62)E−20	–	–
14	3491.452437	3.413(55)E−20	–	–
15	3492.133309	3.384(44)E−20	–	–
16	3492.803678	3.439(31)E−20	0.0817(33)	–
17	3493.463542	3.451(34)E−20	0.0819(29)	0.0703(29)
18	3494.112898	3.408(17)E−20	0.0799(22)	0.0690(22)
19	3494.751744	3.339(14)E−20	0.0789(22)	0.0678(23)
20	3495.380077	3.269(26)E−20	0.0798(24)	0.0684(23)
21	3495.997896	3.187(22)E−20	0.0784(26)	0.0668(28)
22	3496.605198	3.041(26)E−20	0.0782(27)	0.0662(32)
23	3497.201981	2.952(18)E−20	0.0761(20)	0.0648(23)
24	3497.788244	2.751(14)E−20	0.0766(26)	0.0646(28)
25	3498.363984	2.607(15)E−20	0.0762(22)	0.0645(24)
26	3498.929201	2.459(10)E−20	0.0754(17)	0.0637(19)

Table 2 (continued)

m	ν, cm^{-1}	S, $cm^{-1}/(molecules \cdot cm^{-2})$	$\gamma^0(N_2)$, cm^{-1}/atm	$\gamma^0(O_2)$, cm^{-1}/atm
27	3499.484073	2.299(12)E–20	0.0753(20)	0.0634(24)
28	3500.029699	2.064(24)E–20	0.0764(26)	0.0644(28)
29	3500.561397	1.981(8)E–20	0.0740(17)	0.0623(20)
30	3501.084707	1.809(12)E–20	0.0741(20)	0.0624(23)
31	3501.597389	1.666(12)E–20	0.0737(19)	0.0621(24)
32	3502.099440	1.526(8)E–20	0.0739(13)	0.0625(15)
33	3502.590962	1.379(8)E–20	0.0731(16)	0.0618(21)
34	3503.071954	1.248(12)E–20	0.0738(11)	0.0624(20)
35	3503.542636	1.113(9)E–20	0.0726(17)	0.0613(26)
36	3504.002627	9.933(82)E–21	0.0724(13)	0.0615(19)
37	3504.452139	8.791(61)E–21	0.0716(14)	0.0606(22)
38	3504.891112	7.793(80)E–21	0.0718(17)	0.0607(25)
39	3505.319596	6.833(69)E–21	0.0715(12)	0.0613(15)
40	3505.737573	5.992(46)E–21	0.0716(14)	0.0608(18)
41	3506.145224	5.210(42)E–21	0.0713(12)	0.0607(16)
42	3506.542291	4.526(68)E–21	0.0708(13)	0.0613(17)
43	3506.929124	3.904(56)E–21	0.0709(8)	0.0614(16)
44	3507.305996	3.216(82)E–21	0.0689(2)	0.0587(3)
45	3507.675229	2.822(43)E–21	0.0698(18)	0.0605(21)
46	3507.996825	2.043(65)E–21	0.0697(11)	0.0611(8)
47	3508.361768	2.040(30)E–21	0.0695(7)	0.0601(14)
48	3508.697869	1.764(39)E–21	0.0704(8)	0.0616(30)
49	3509.021803	1.485(48)E–21	0.0701(16)	0.0627(28)
50	3509.335023	1.235(0)E–21	0.0729(28)	0.0664(112)
51	3509.637472	1.047(0)E–21	0.0752(37)	0.0705(167)
52	3509.929305	8.552(350)E–22	0.0682(2)	0.0625(0)
53	3510.210676	7.092(357)E–22	0.0673(13)	0.0632(28)
54	3510.481420	5.671(398)E–22	0.0657(26)	0.0627(31)

* 5.497Å–22 should be read as $5.497 \cdot 10^{-22}$, others similarly.

2. The squared transition dipole moment and the Herman–Wallis factor

Figure 2 shows the variation of the squared transition dipole moments with quantum number m for the $\nu_1 + \nu_3$ band of $^{14}N_2{}^{16}O$. The squared transition dipole moments in this study were in good agreement with the values calculated using the line strengths of HITRAN92,[2] though a small difference between our values and the HITRAN92 values was found. In the HITRAN92 database, the Herman–Wallis factor was not considered, and the sudden depletion of the line strengths at $m = -47$, -29, 28, and 46 was not appeared. On the other hand, in the HITRAN2K database, the Herman–Wallis factor is included in the calculation of line strengths and the sudden depletion of the line strengths at $m = -47$, -29, 28, and 46 is distinct. Almost the same sudden depletion of the line strengths is found in our data. Column 2 in Table 3 shows the comparison of the square of the transition dipole moment matrix element in this study together with other experimental results for the $\nu_1 + \nu_3$ band of $^{14}N_2{}^{16}O$. Our values are very close to the value reported by Regalia et al.[8]

The linear and quadratic coefficients of the Herman–Wallis factor were derived from the transition dipole moment using the least-squares method. Columns 3 and 4 in Table 3 show the linear and quadratic coefficients of the Herman–Wallis factor for the $\nu_1 + \nu_3$ band of $^{14}N_2{}^{16}O$, respectively. It should be stressed that even if these coefficients are used to calculate the line strengths and/or the squared transition dipole moments, the calculated values at $m = -47$, -29, 28, and 46 are largely deviated from the experimental data. The signs of the

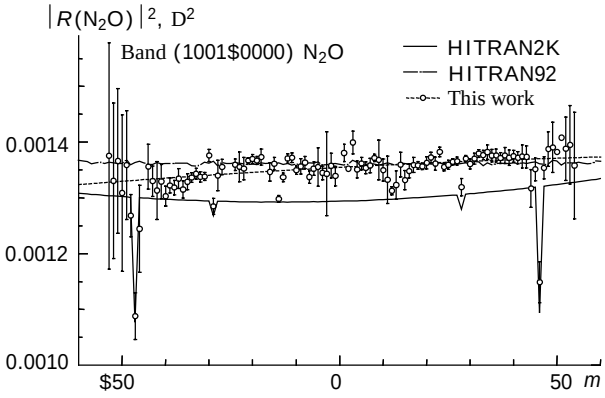

Fig. 2. Variation of the squared transition dipole moment with rotational quantum number m for the $\nu_1 + \nu_3$ band of $^{14}N_2{}^{16}O$.

Table 3. The square of the transition dipole moment matrix element and the coefficients of the Herman–Wallis factor for the $\nu_1 + \nu_3$ band of $^{14}N_2{}^{16}O$

Reference	$\lvert R_V(N_2O)\rvert^2$ ($\times 10^{-3}$ D^2)	$A_1 \cdot 10^{-4}$	$A_2 \cdot 10^{-6}$
5	1.184 ± 0.051	1.85	–3.9
6	1.317 ± 0.067	–	–
7	1.292 ± 0.009	0.8	2.9
8	1.354 ± 0.014	0.8	–2.84
This work	1.355 ± 0.002	1.53	–0.637

quadratic coefficients of the Herman–Wallis factor in this study were similar to the results by Toth[5] and Regalia et al.,[8] however, the recent results obtained by Toth[7] have opposite sign to ours.

3. N_2- and O_2-broadened half-widths

Figures 3 and 4 show the N_2- and O_2-broadened half-widths of the *R*- and *P*-branch lines, respectively. There were no systematic differences between the half-widths in both branches. The N_2- and O_2-broadened half-widths obtained in this study were in excellent agreement with the recent high-resolution experiments reported by Henry et al.,[12] Toth,[13] and Nemtchinov et al.[14] The N_2- and O_2-broadened half-widths reported by Lacome et al.,[11] which are the basic data of the air-broadened half-widths in the HITRAN database, agreed well with the recent high-resolution experiments and our results beyond $|m| = 12$, while their data were a few percent lower than our results below $|m| = 12$. The previous values reported by Toth[9] and Margolis[10] were 4–5% larger than our results for the N_2-broadened half-widths.

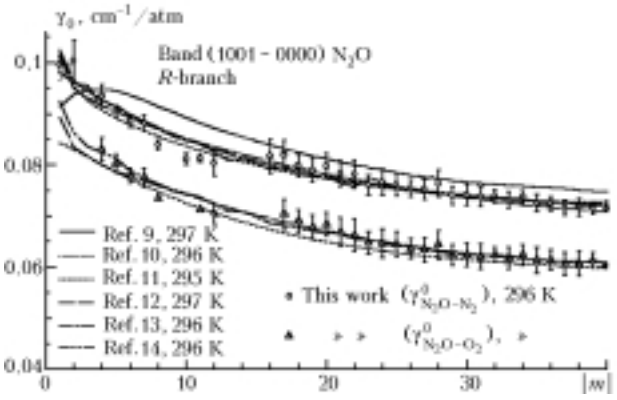

Fig. 3. N_2- and O_2-broadened half-widths of *R*-branch lines in the $\nu_1+\nu_3$ band of $^{14}N_2{}^{16}O$.

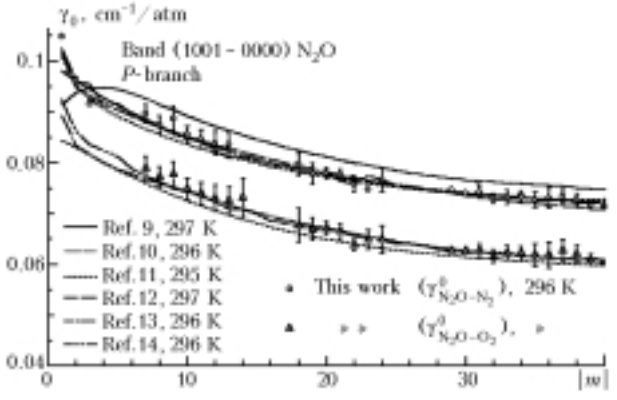

Fig. 4. N_2- and O_2-broadened half-widths of *P*-branch lines in the $\nu_1+\nu_3$ band of $^{14}N_2{}^{16}O$.

Smoothed half-widths were determined by a cubic polynomial fit

$$\gamma^0(N_2O - X) = a_0 + a_1 M + a_2 M^2 + a_3 M^3, \quad (5)$$

where $M = |m|$, X is the buffer gas (N_2 or O_2). The coefficients of the above cubic polynomial determined from the experiments are listed in the second and third columns of Table 4 for the N_2- and O_2-broadened half-widths, respectively. These coefficients were determined by the least squares fitting of the lines for $|m| = 1$ to $|m| = 40$.

Table 4. Coefficients derived for smoothed values of the N_2-, O_2-, and air-broadened half-widths

Coefficient	N_2	O_2	Air
a_0	0.1039	0.08958	0.1009
a_1	−0.002726	−0.001962	−0.002564
a_2	8.661E−5*	5.016E−5	7.883E−5
a_3	−9.694E−7	−4.866E−7	−8.659E−7

* 8.661Å–5 should be read as $8.661 \cdot 10^{-5}$, others similarly.

4. Air-broadened half-widths

In order to compare with the HITRAN databases, air-broadened half-widths were derived from the smoothed values of $\gamma^0(N_2O\text{-}N_2)$ and $\gamma^0(N_2O\text{-}O_2)$ using the following expression

$$\gamma^0(N_2O - \text{air}) = 0.79\,\gamma^0(N_2O - N_2) + \\ + 0.21\,\gamma^0(N_2O - O_2). \quad (6)$$

Coefficients of the cubic polynomial for the smoothed air-broadened half-widths were listed in the fourth column of Table 4. The calculated air-broadened half-widths are in good agreement with the values of HITRAN2K beyond $|m| = 12$, while the air-broadened half-widths in this study are about 4% larger than those of HITRAN2K around $|m| = 3$.

Conclusions

Line strengths, N_2-, and O_2-broadened half-widths in the $\nu_1+\nu_3$ band of $^{14}N_2{}^{16}O$ were determined from spectra obtained by a high-resolution Fourier transform spectrometer at room temperature. The line strengths obtained in this study agreed with the values of HITRAN92[2] rather than those of HITRAN96[3] and HITRAN2K.[4] The square of the transition dipole moment matrix element and the coefficients of the Herman–Wallis factor were also determined for this band. The square of the transition dipole moment matrix element in this study was in excellent agreement with the recent high-resolution experiment by Regalia et al.[8] The N_2- and O_2-broadened half-widths measured in this study were in good agreement with the values of the recent high-resolution experiments reported by Henry et al.,[12] Toth,[13] and Nemtchinov et al.[14] Air-broadened half-widths were derived from the N_2- and O_2-broadened half-widths smoothed by a cubic polynomial fit. These results will contribute to the improvement of the accuracies of the spectroscopic databases and will be useful for remote sensing measurements of N_2O

and atmospheric temperature, and the studies of the thermal balance in the terrestrial atmosphere.

References

1. R.A. McClatchey, W.S. Benedict, S.A. Clough, D.E. Burch, R.F. Calfee, K. Fox, L.S. Rothman, and J.S. Garing, *AFCRL Atmospheric Absorption Line Parameters Compilation*, AFCRL–TR–0096, AFCRL, Bedford, MA (1973).
2. L.S. Rothman, R.R. Gamache, A. Goldman, L.R. Brown, R.A. Toth, H.M. Pickett, R.L. Poynter, J.-M. Flaud, C. Camy-Peyret, A. Barbe, N. Husson, C.P. Rinsland, and M.A.H. Smith, *The HITRAN database: 1986 Edition*, Appl. Opt. **26**, 4058–4097 (1987).
3. L.S. Rothman, R.R. Gamache, R.H. Tipping, C.P. Rinsland, M.A.H. Smith, D. Chris Benner, V. Malathy Devi, J.-M. Flaud, C. Camy-Peyret, A. Perrin, A. Goldman, S.T. Massie, L.R. Brown, and R.A. Toth, *The HITRAN molecular database: Edition of 1991 and 1992*, J. Quant. Spectrosc. Radiat. Transfer **48**, 469–507 (1992).
4. L.S. Rothman, C.P. Rinsland, A. Goldman, S.T. Massie, D.P. Edwards, J.-M. Flaud, A. Perrin, C. Camy-Peyret, V. Dana, J.-Y. Mandin, J. Schroeder, A. Mccann, R.R. Gamache, R.B. Wattson, K. Yoshino, K.V. Chance, K.W. Jucks, L.R. Brown, V. Nemtchinov, and P. Varanasi, *The HITRAN molecular spectroscopic database and HAWKS (HITRAN atmospheric aorkstation): 1996 Edition*, J. Quant. Spectrosc. Radiat. Transfer **60**, 665–710 (1998).
5. R.A. Toth, *Line Strengths of* N_2O *in the* 2.9 micron *region*, J. Quant. Spectrosc. Radiat. Transfer **40**, 588–604 (1971).
6. R.H. Kagann, *Infrared absorption intensities for* N_2O, J. Mol. Spectrosc. **95**, 297–305 (1982).
7. R.A. Toth, *Line strengths* (900–3600 cm^{-1}), *self-broadened linewidths, and frequency shifts* (1800–2360 cm^{-1}) *of* N_2O, Appl. Opt. **32**, 7326–7365 (1993).
8. L. Regalia, X. Thomas, A. Hamdouni, and A. Barbe, *Intensities of* N_2O *measurements in the* 4 *and* 3 μm *region using Fourier transform spectrometer*, J. Quant. Spectrosc. Radiat. Transfer **57**, 435–444 (1997).
9. R.A. Toth, *Self-broadened and* N_2 *broadened linewidths of* N_2O, J. Mol. Spectrosc. **40**, 605–615 (1971).
10. J.S. Margolis, *Intensity and half width measurements of the* ($00^02–00^00$) *band of* N_2O," J. Quant. Spectrosc. Radiat. Transfer **12**, 751–757 (1972).
11. N. Lacome, A. Levy, and G. Guelachvili, *Fourier transform measurement of self-,* N_2*-, and* O_2*-broadening of* N_2O *lines: temperature dependence of linewidths*, Appl. Opt. **23**, 425–435 (1984).
12. A. Henry, M. Margottin-Maclou, and N. Lacome, N_2*- and* O_2*-broadening parameters in the* ν_3 *band of* $^{14}N_2{}^{16}O$, J. Mol. Spectrosc. **111**, 291–300 (1985).
13. R.A. Toth, N_2*- and air-broadened linewidths and frequency-shifts of* N_2O, J. Quant. Spectrosc. Radiat. Transfer **66** 285–304 (2000).
14. V. Nemtchinov, P. Varanasi, and C. Sun, *Measurements of line intensities and line widths in the* ν_3*-fundamental band of nitrous oxide at atmospheric temperatures*, J. Quant. Spectrosc. Radiat. Transfer, (in press).
15. L.D.G. Young, *Calculation of the partition function for* $^{14}N_2{}^{16}O$, J. Quant. Spectrosc. Radiat. Transfer **11**, 1265–1270 (1971).